Design and construction of a focal plane slicing mirror

Demetrio Magrin[a], Enrico Giro[a], Favio Bortoletto[a], Giuseppe Crimi[b], Claudio Pernechele[c], Raffaele Tomelleri[d]
[a]INAF – Osservatorio Astronomico di Padova, Vicolo dell'Osservatorio 5, 35122 Padova, Italy
[b]INAF – Osservatorio Astronomico di Brera, sede di Merate, via E. Bianchi 46, 23807 Merate (LC), Italy
[c]INAF – Osservatorio Astronomico di Cagliari, Loc. Poggio dei Pini, Strada 54 09012 Capoterra (CA), Italy
[d]Tomelleri Srl – Viale Del Lavoro,12/A, 37069 Villafranca Di Verona, Italy

ABSTRACT

We describe here the optical design, mechanical project and the manufacturing of a mechanically reconfigurable spherical slicing mirror. We made use of nowadays commonly available mechanical cutting techniques (wire spark-erosion) to obtain single blades (slices) shaped with profile close to the optical sag specification. Blades so constructed are ready to be optically finished with standard optical workshop techniques. We present here the results obtained from metrology made on the first constructive phase of the system before to start the final optical polishing phase.

Keywords: slicing mirror, integral field unit, mechanics, optics, metrology.

1. INTRODUCTION

The aim of the Integral Field Spectroscopy (IFS) is to provide the spatial and the spectral information over an extended portion of the sky by optical subdivision and multiplexing of the same. The basics of this observation technique and the possibilities for developing conventional IFS have been largely explored and can be divided in three different kinds of approaches following the nature of the optical element used as field sub-divider:

- The use of a two-dimensions lenslet array [1][2]
- The use of a two-dimensional lenslet array coupled to a fibre-bundle [3]
- The use of an image slicing mirror array [4]

All three designs are based on a traditional spectrograph where the field of interest of the telescope focal plane is dissected and relayed to spectrograph input slit. In this fashion the slicer can be viewed as a removable optical unit (Integral Field Unit, IFU) realizing a retrofit of a previously available spectrograph. The first two concepts differs basically in the way to multiplex the resulting slicing spectra on the spectrograph final detector allowing different optimizations in terms of detector surface usage, sky sampling and overall throughput. The third concept allows the construction of a full reflective slicing unit or hybrid in that the critical part, the slicer, is reflective and the slit re-imaging optics is refractive. The field of interest is in this case subdivided in one dimension by the reflecting facets composing the slicer, the second spatial dimension is recovered from the natural spectrograph spatial coordinate orthogonal to dispersion. A further differentiation among mirror slicers is between plane and spherical slicer facets, the first case providing easier manufacturing and the second easier optical alignment of facets [5].

The present paper is concerned with the optical design and mechanical construction of spherical mirror-slicers. In the framework of the OPTICON JRA5 activity we experimented the possibility to replicate slicing-mirrors starting from monolithic aluminum and zerodur negative mandrels constructed by diamond-turning machining.

Replication has been attempted both with nickel galvanic deposition and SiC plasma enhanced chemical vapor deposition (PECVD) [6]. This technique allows in principle the possibility to produce an high number of similar pieces but at the expense of long experimentation trials in order to minimize the deformations induced on replicas by temperature gradients and electric-field disuniformities on the mandrel surface. The present work is concerned with the

Advanced Optical and Mechanical Technologies in Telescopes and Instrumentation, edited by Eli Atad-Ettedgui, Dietrich Lemke, Proc. of SPIE Vol. 7018, 701837, (2008) · 0277-786X/08/$18 · doi: 10.1117/12.787550

construction of a single spherical slicer made by separated metallic plates shifted and fixed with the off-sets imposed at optical design phase. This mechanical technique [5] proceeds basically in two steps:

- Spherical optical machining is made with slices packaged shifting them to match the reference marks previously drilled on the slices themselves
- Packaging of slices for operation making use of a different set of reference marks

The operation is based on simple lateral shifts of the slices inserted on a reference cage, this comes from the spherical design. The two sets of marks are created during the slices spark-erosion cut. This technique produces non monolithic slicers but with the advantage to be affordable with workshop machinery easily available. The choice of the material used for this purpose was STAVAX, an iron-based alloy often used for plastic molds and with high surface finish properties (surface hardness, 200 HB).

2. OPTICAL DESIGN

In order to start with an optical design we considered as a possible target application the DOLORES spectrograph [7] mounted and operative at the Nasmyth B of the Telescopio Nazionale Galileo (TNG, La Palma) and, in particular, the optical configuration proposed by [8] for an extension to 3D spectroscopy capability.

The Dolores camera is a F/3.2 and mounts a Loral thinned back-illuminated CCD with format 2048×2048 and pixel size of 15 μm. The plate factor is 0.275 arcsec/pixel giving a field of view of about 9.4×9.4 arcsec^2. Dolores allows different observing modes like direct imaging, long slit spectroscopy and multi object spectroscopy over a wavelength range 300 – 1000 μm. The dispersing elements (single and multiple order) are hosted on a grism wheel (containing also Volume Phase Holographic Gratings) allowing to select the resolution from 500μm to 2500μm with different central wavelengths. Slits are carried by a slider located at the telescope focal plane.

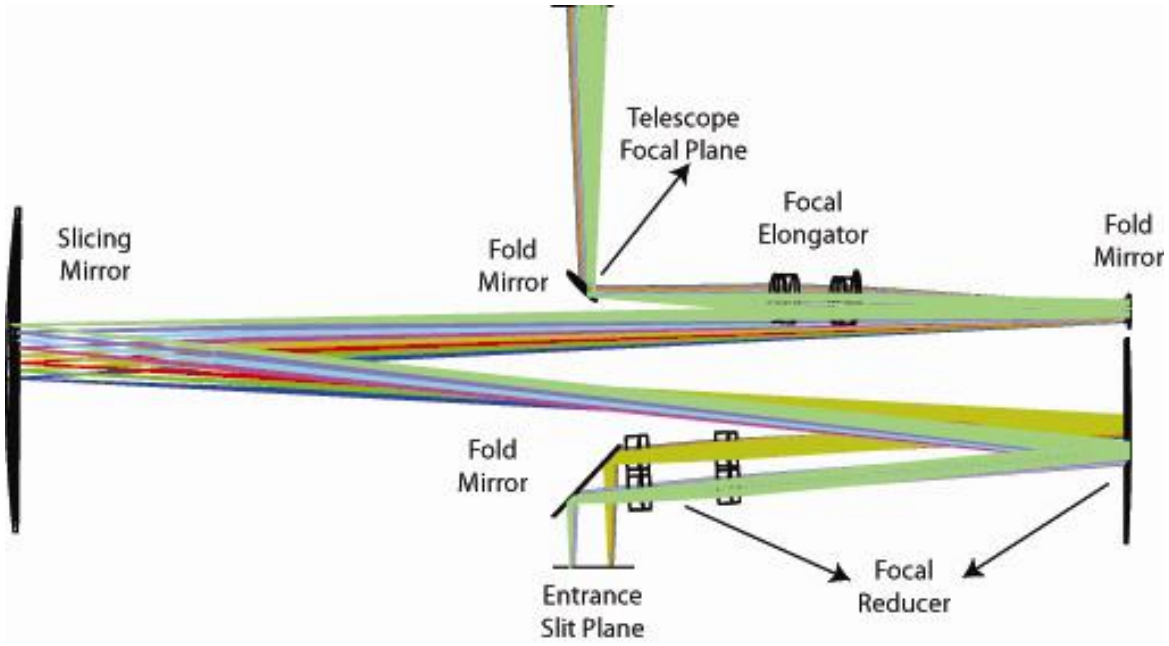

Fig. 1 A complete 'focal-plane to focal-plane' view for the proposed IFU.

The IFU optical layout here proposed is shown in Fig. 1. It is very similar to those for UKIRT and MIRI on JWST [5]; the only modification is in the refractive design of the re-imaging section selected in our case. In order to have a removable system the IFU, when inserted, will trap the telescope optical beam to perform the image splitting and will project the resulting *slices* on the spectrograph focal plane preserving the main telescope beam parameters. A mirror on the focal plane splits the field of view in two identical channels (only one channel is shown in Fig. 1) so allowing the accommodation of an identical second slicing mirror to completely fill the available detector area (16 plus 16 slices in the considered case). The first element in the optical path is a refractive focal elongator which reforms the focal plane at the desired scale on the slicing mirror. The slicing mirror directs the light onto a refractive focal reducer (one for each slice) that rescales the focal plane in the entrance slit plane of DOLORES and reproduces each sliced image seen from the spectrograph optics with the same, common, exit pupil as in the non-IFU mode, so after the IFU insertion only a 5 cm shift of the focal plane has to be commanded to the telescope secondary mirror .

2.1 Slicing mirror dimensioning

The optical design for the reconfigurable slicing mirror has being carried out by considering a paraxial approximation for the focal elongator and the focal reducer. A scheme of the considered optical layout with the principal planes spot diagrams is shown in **Error! Reference source not found.**.

The image slicing mirror has been simulated in ZEMAX with both multi-configurations capability and making use of the *SlicerMirrorArray* routine developed by [9]. The assumed slice width was of 1 mm, a good compromise between machining constrains and sampling requirements. The resulting projected angular dimension is 0.55 arcsec (2 pixel sampling with the DOLORES scale of 0.275 arcsec/pixel).

Given the DOLORES field of view (563×563 arcsec^2), it is then possible to cover the whole detector with 32 slices having a length of 17.6 arcsec (32 mm). This means that the 3D capability could be ideally applied to a field of view 17.6×17.6 arcsec^2. To avoid crosstalk effects, we have considered a separation between the images of each slice of 4 pixels, corresponding to 1.1 arcsec at the entrance slit. The field of view along the spatial direction of the spectrograph is defined by a dekker as usual.

A focal elongator is placed 30 mm after the TNG focal plane (entrance pupil size 3600 mm, effective focal length 39600 mm) and converts the telescope F/11 to about F/104 to reform the focal plane at the right scale on the slicing mirror. The pupil illuminating the slicer will appear at about 27.15 mm from the focal elongator and the re-imaged focal plane at 256.96 mm afterwards (see Fig. 2). The slicing mirror is formed by 16 slices ideally obtained from a common spherical mirror whose radius of curvature is 256.96 mm. In this way, each slice reforms the image of the pupil at the same distance from the slicing mirror but laterally displaced to produce separate pupil images. At 27.15 mm from each slicer produced pupil, a set of refractive focal reducers (one for each slice) recovers the original telescope focal beam.

The resulting single slice radius of curvature is 256.96 mm and projected pupil size is 2.463 mm.

Table 1. Shift in the spectrograph spatial and dispersing directions applied to the slices after machining. Units are mm.

# Slice	1	2	3	4	5	6	7	8
Shift in the non-dispersion direction	1.624	-4.871	8.118	-11.365	14.612	-17.860	21.107	-24.354
Shift in the dispersion direction	2.000	2.000	2.000	2.000	2.000	2.000	2.000	2.000
# Slice	9	10	11	12	13	14	15	16
Shift in the non-dispersion direction	24.354	-21.107	17.860	-14.612	11.365	-8.118	4.871	-1.624
Shift in the dispersion direction	-2.000	-2.000	-2.000	-2.000	-2.000	-2.000	-2.000	-2.000

The spatial dispersion of slices at the entrance slit in the spectrograph (spectrograph spatial direction) is obtained by lateral displacement of each slice. A further improvement in system compactness is obtained by inserting a fixed separation between the slices in the dispersion direction (see section 3). This trick separates the slicing mirrors in two sets of eight slices laterally shifted along the dispersion direction; this allows a very compact (refractive) focal reducer, avoiding overlaps among the pupils. The introduced shift between the two sets has an absolute value of 4 mm, corresponding to 2.1 arcsec in the sky.

The relative shifts applied to each slice from the original machining position are reported in Table 1.

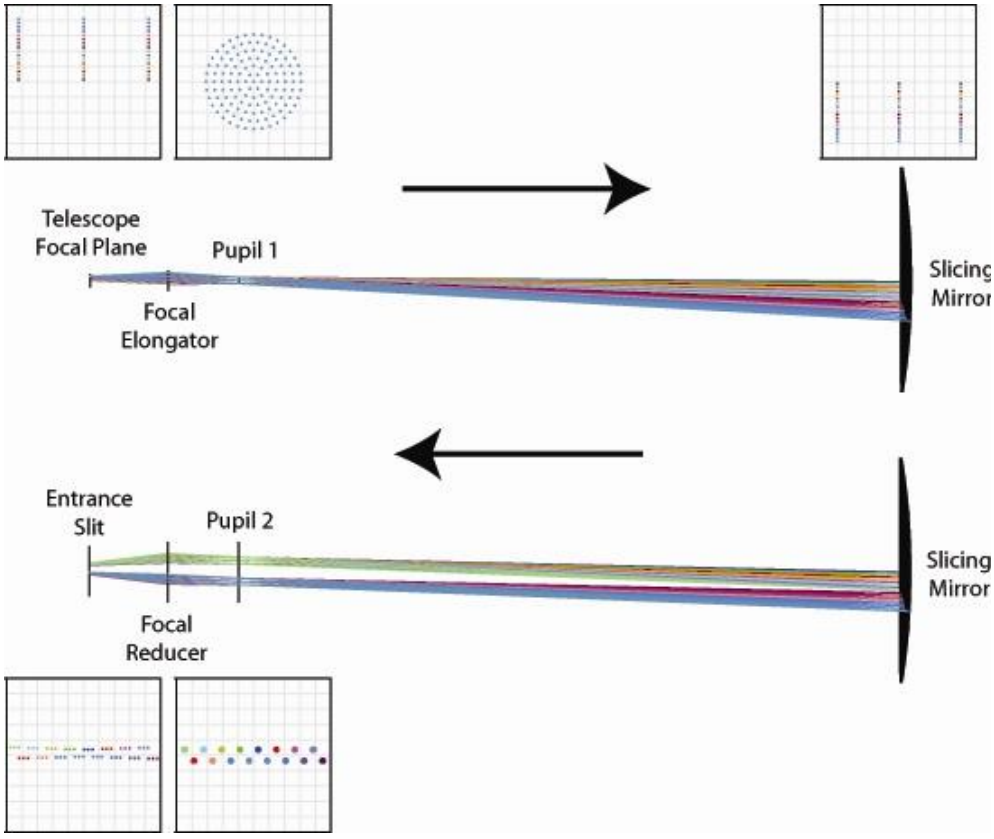

Fig. 2 First order optical layout for the relevant IFU optical planes.

2.2 Tolerances on slices positioning

Positioning errors on slicers produce misplacement errors on the final slices images and pupils. The position of a pupil after a slicing mirror is controlled by its position angle. Assuming an acceptable pupil position/size error of 1%, the acceptable error on the slice relative displacement is 12 μm corresponding to a tilt of 0.046 mrad. Also the errors on the slice lateral position could generate overlapping between the final images; fortunately this effect is consistently reduced by the de-magnification ratio between the focal plane at the image slicing mirror and the focal plane at the entrance slit plane of about 0.1. It is to be noted that this error is reflected in a stable off-set in the dispersion direction, so adjustable, slice per slice, after the usual wavelength calibration performed with a spectra calibration lamp.

An error in the slice width linearly transforms into an error in the resolution. We assume here an acceptable error of 1% between slices width.

Errors in the slice length are neglected considering that, in the final operational configuration (see Fig. 3), only a portion of the reflecting surface formed by the sandwich will be interested by the incoming light beam.

3. MECHANICAL DESIGN AND MANUFACTURING

The image slicing mirror has been thought as reconfigurable, i.e. the same cage-holder is to be used for machining and operation [5] so facilitating the construction process. To get this feature the slices can be placed in two possible configurations inside the iron cage:

- Optical surface machining. The grossly-machined slices are pressed together and optically finished to a common spherical sag with the required radius of curvature. During this operation, a spacer is inserted between the two set of slices allowing the decoupling of the pupils in the operational configuration.
- Operational configuration. The spacer is removed, the slices are stacked maintaining the same order and, one by one, laterally shifted to the right position. Apart from constructive errors this configuration will produce the correct set of pupils to be imaged by the re-imaging optics on the spectrograph slit plane.

The right alignment of the sixteen slicing mirrors in the two configurations is made possible by the use of two sets of holes placed at the shifting edge of each slice. When the first set of holes is aligned by an inserted spindle we have the first configuration, the 'operational' is obtained when the second set of holes is aligned by a different spindle. The two basic configurations are shown in Fig. 3.

With this constructive technique the positioning errors are in fact determined by the accuracy in the relative distance between the two holes in each slice and by the repeatability of the slice alignment along each set of holes which means to use spindles verified for dimensional uniformity.

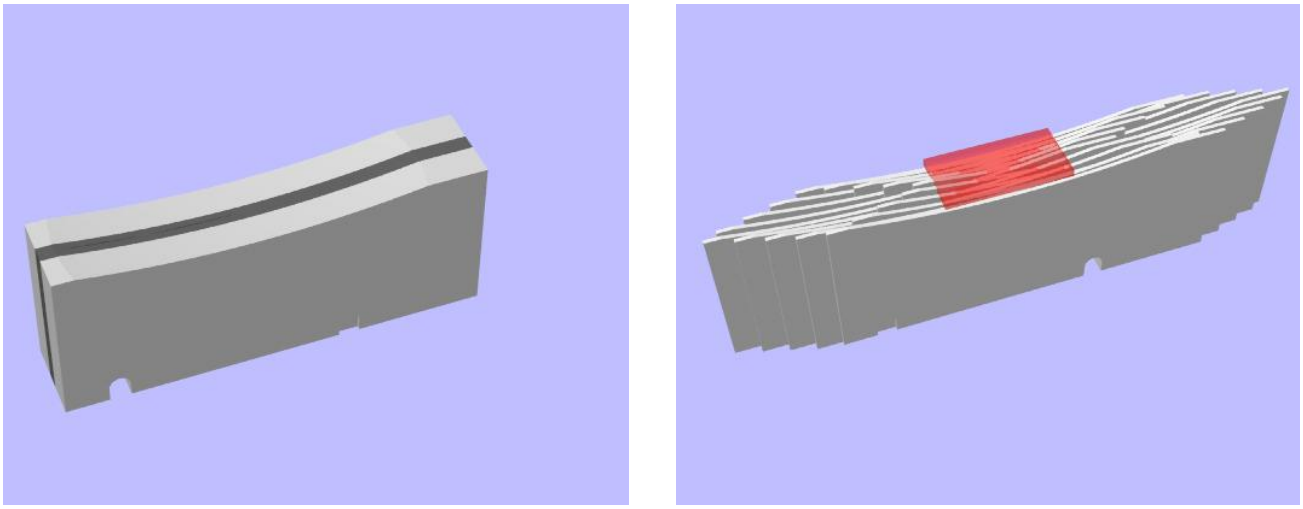

Fig. 3 View of the sixteen slicing mirrors in the "manufacturing" configuration (left) and in the "operational" configuration (right). The passing-through holes for the spindle aligner are also visible in the two basic configurations. The illuminated working area of the slicer is delimited in the right view.

The useful slicing mirror area is superimposed in the right figure and corresponds to 16×32 mm^2. Looking at the figure, it is clear that this constructive method inherently produces slices with a redundant length, in our case each slice is 99.6 mm in length.

In practice the most critical constructive phase is the preparation of the single stavax iron slices. This has been done in three machining steps:

- Cut of rectangular pieces with a wire spark-erosion machine from a block of stavax
- Creation with the same technique of reference holes and rough spherical sag
- Precision grinding of the two, flat, lateral surfaces at the required quote

The cage-box shown in Fig. 4 has been constructed with a milling machine and grinding the reference surfaces.

Fig. 4 Left: view of the 16 slices ready to be inserted on the cage-box for optical finishing. The reflecting side has been pre figured during the spark-erosion cut. The central piece is the spacer to be used only during optical finishing. Right: the slices and spacer inserted on the cage-box.

4. MEASUREMENT

Single slices have been made individually, therefore there can be a variation in their nominal thickness (value 1 mm) although minimized by grinding of lateral surfaces. Each slice thickness has been measured in four separated points with a micrometer obtaining a mean value of 1.002 mm with a standard deviation of 0.003 mm, less than 1% of the nominal thickness. Possible non-planarities of the slices have not been considered because both in optical finishing and operational configurations slices are packaged and pressed laterally to form a sort of monolithic block

Positioning errors, exchanging the two configurations, have been estimated by measuring, slice by slice, the distances between the left facets and right facets of the couple of reference holes. Measures have been obtained with the help of a 3D coordinate measuring machine provided with a reference touching finger. This system has been proved to deliver an average accuracy of 3 μm.

A comparison with the values obtained from the optical project and shown in Table 1 requires a rearrangement of the measured quantities of Table 2 by subtraction of a common off-set estimated from the optical design of 39.341 mm.

This is equivalent to a lateral shift of the entire image slicing sandwich, i.e. to shift the zero-point of the lateral coordinate, or, equivalently to a shift in the non-dispersion direction applied to all the slices images in the focal plane. This is shown in Table 3 and allows a direct comparison with the model (Table 1) with results shown in Fig. 5.

The RMS error on the reference marks position for the whole group of slices is 10 μm. Looking at Fig. 5 we can see that the large majority of slices is well below the mechanical constraints imposed by the optical project, with the exception of a few slices at the limit of acceptance. Being this the first practical attempt to mechanically build such a kind of high precision piece we believe it can be considered an encouraging result.

Table 2. Measurements of the distances between the left sides and the distances between the right side of the two holes for each slice. Units are millimeters.

# Slice	1	2	3	4	5	6	7	8
differences (left sides)	40.965	34.471	47.440	27.979	53.994	21.505	60.439	14.996
differences (right sides)	40.968	34.471	47.440	27.973	53.931	21.510	60.434	14.990
# Slice	9	10	11	12	13	14	15	16
differences (left sides)	63.692	18,234	57.201	24.730	50.706	31.233	44.212	37.715
differences (right sides)	63.680	18.222	57.195	24.730	50.706	31.229	44.207	37.732

Table 3. Expected shift in the non-dispersion direction for each slice. Units are millimeters.

# Slice	1	2	3	4	5	6	7	8
shift (left sides)	1.624	-4.870	8.099	-11.362	14.653	-17.836	21.098	-24.345
shift (right sides)	1.627	-4.870	8.099	-11.368	14.590	-17.831	21.093	-24.351
# Slice	9	10	11	12	13	14	15	16
shift (left sides)	24.351	-21.107	17.860	-14.611	11.365	-8.108	4.871	-1.626
shift (right sides)	24.339	-21.119	17.854	-14.611	11.365	-8.112	4.866	-1.609

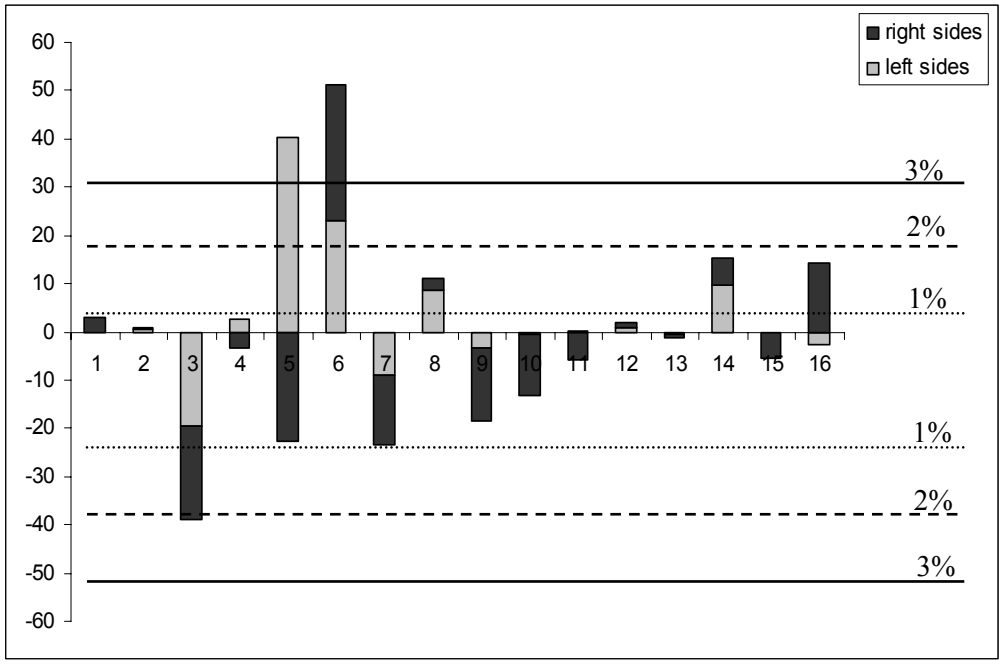

Fig. 5 Expected errors (μm) on lateral displacements for each slice. Horizontal lines represent the corresponding percentage of error in the projected pupil position relative to the nominal pupil diameter.

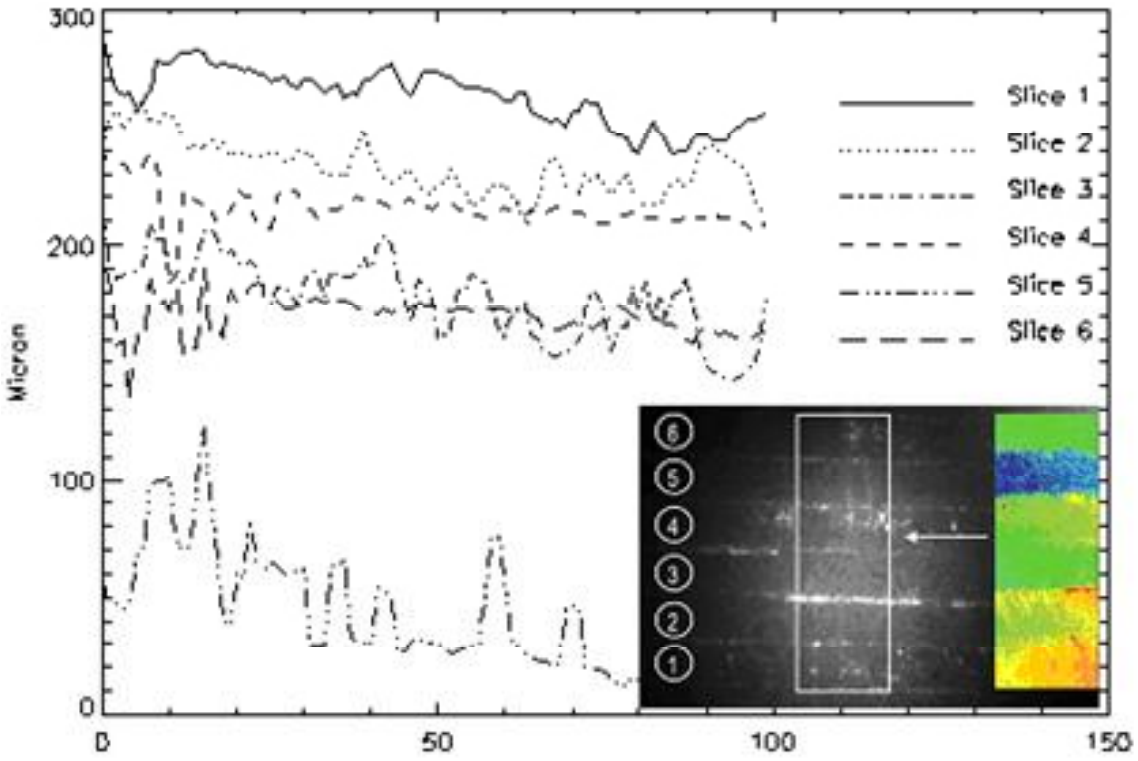

Fig. 6 Roughness profiles obtained along six slices with the OCT interferometric measurement.

The last measurement was aimed in obtaining an estimate of the surface roughness delivered by the spark-erosion cut technique largely used in this experiment. It has been done using a common OCT (optical coherence tomography) interferometric arrangement making use of a partially coherent source (SLED working @820 nm), a reference reflecting surface (a $\lambda/8$ flat mirror) mounted on a precision shift stage and a CCD camera.

The light scattered by the rough surface is imaged through an objective into the CCD area after interfering with the beam coming from the reference mirror. CCD acquisitions are synchronized with the measured movement of the mirror allowing an a-posteriori retrieval of the 3-D surface as described in [10].

A view of the profile along six staked slices aligned in optical finishing mode is shown in Fig. 6. The region examined is the wire spark-erosion cut on the edges to be optically machined, the lateral size of the scan is 2.5 mm as seen in the OCT picture shown in Figure 6. The spatial sampling on the camera is 25 micron/pixel and the surface roughness is estimated to be less than 20 microns RMS.

5. CONCLUSIONS

The optical design of a reconfigurable IFU to be used with an already available spectrograph has been made. The mechanical construction of the most critical part, the slicing mirror, has been terminated and was obtained with standard workshop techniques; extended metrology made on the slicer shows a good compatibility with the expected error budget. We expect now to perform the final optical polishing of surfaces and to complete the IFU with the transmissive re-imaging optical system.

REFERENCES

[1] Bacon, R., Adam, G., Baranne, A., Courtes, G., Dubet, D., Dubois, J.P., Georgelin, Y., Monnet, G., Pecontal, E., Urios, J.,"The integral field spectrograph TIGER", Proceedings of the ESO Conference on VLTs and their Instrumentation, Munich (1988).

[2] Giro, E., Claudi, R.U., Antichi, J., Bruno, P., Cascone, E., De Caprio, V., Desidera, S., Gratton, R.G., Mesa D., Scuderi, S., Turatto, M., Beuzit, R.U., Puget, P. "BIGRE: a new double microlens array for the integral field spectrograph of SPHERE", Proc. SPIE at this conference (2008).

[3] Allington-Smith, J., Murray, G., Content, R., Dodsworth, G., Davies, R., "Integral Field Spectroscopy with the Gemini Multiobject Spectrograph. I. Design, Construction, and Testing", PASP, 114, 892–912 (2002).

[4] Bowen, I.S. , "'The image slicer, a device for reducing loss of light at slit of stellar spectrograph", Ap. J., 88, 113 (1938).

[5] Wells, M., Hastings, P.R., Ramsay-Howat, S.K., "Design and testing of a cryogenic image slicing IFU for UKIRT and NGST",Proc. SPIE, 4008, 1215-1226 (2000).

[6] Schmoll, J., Robertson, D.J., Dubbeldam, C.M., Yao, J., Bortoletto, F., Pina, L., Hudec. R., Prieto, E., Norrie, C., Ramsay-Howat,S., Preuss, W., "Optical replication techniques for image slicers", New Astron. Rev., 50, 263-266 (2006).

[7] Conconi, P., et alt, "Dolores: the low-resolution optical imager and spectrograph", Proc. CNAA-INAF Meeting, La Palma (Canary Islands), 158-161 (2000).

[8] Mazzoleni, R., Zerbi, F.M., Held, E.V., Ciroi, S., Conconi, P., Fernandez-Soto, A., Franceschini, A., Guzzo, L., Molinari, E., Rafanelli, P., Rizzo, D. and Rizzi, L. "Retrofitting focal reducer spectrographs with removable integral field units", Proc. SPIE, 4842, 219-230 (2003).

[9] Vives, S., Prieto, E., Moretto, G., and Saisse, M. "Modeling a slicer mirror using Zemax user-defined surface", New Astronomy Review, 50, 271-274, (2006).

[10] Jahanmir, J. and Wyant, J.C. "Comparison of surface roughness measured with an optical profiler and a scanning probe microscope (Invited Paper)", Proc. SPIE, 1720, 111-118, (1992).